# ELASTIC SCATTERING OF $^{58}$Ni + $^{64}$Ni NEAR THE COULOMB BARRIER

A.M. STEFANINI [a], Jincheng XU [a,1], L. CORRADI [a], G. MONTAGNOLI [a], H. MORENO [a,2], Y. NAGASHIMA [a,3], L. MUELLER [a], M. NARAYANASAMY [a,4], D.R. NAPOLI [a,5], P. SPOLAORE [a], S. BEGHINI [b], F. SCARLASSARA [b], G.F. SEGATO [b], F. SORAMEL [b], C. SIGNORINI [c], H. ESBENSEN [d], S. LANDOWNE [d] and G. POLLAROLO [e]

[a] *Istituto Nazionale di Fisica Nucleare, Laboratori Nazionali di Legnaro, I-35020 Legnaro (Padua), Italy*
[b] *Dipartimento di Fisica, Università di Padova, and Istituto Nazionale di Fisica Nucleare, Sezione di Padova, I-35131 Padua, Italy*
[c] *Dipartimento di Fisica, Università di Salerno, I-84100 Salerno, Italy and Istituto Nazionale di Fisica Nucleare, Sezione di Padova, I-35131 Padua, Italy*
[d] *Physics Division, Argonne National Laboratory, Argonne, IL 60439, USA*
[e] *Dipartimento di Fisica Teorica, Università di Torino, I-10125 Turin, Italy and Istituto Nazionale di Fisica Nucleare, Sezione di Torino, I-10125 Turin, Italy*

Received 5 December 1989

Elastic scattering angular distributions have been measured for $^{58}$Ni + $^{64}$Ni at three energies around the Coulomb barrier employing a new kinematic coincidence technique. The data are compared with the results of coupled-channels calculations including inelastic excitations as well as one- and two-neutron transfer reactions. The agreement is good and the calculations also agree well with the available transfer and fusion reaction data.

The measurements of sub-barrier fusion reactions in the system $^{58}$Ni + $^{64}$Ni revealed some years ago [1] large enhancements when compared to the predictions of conventional one-dimensional barrier penetration models, and also showed a relative enhancement with respect to the corresponding data for the symmetric systems $^{58}$Ni + $^{58}$Ni and $^{64}$Ni + $^{64}$Ni. That discovery was compelling evidence for the important role that nuclear structure plays in the low energy fusion process. More recently, in order to obtain more information about the dynamics of the $^{58}$Ni + $^{64}$Ni reaction, transfer cross sections [2,3] and also quasi-elastic scattering angular distributions [3] have been measured.

It has also become clear from other experimental and theoretical studies [4] that dynamical effects manifest themselves in elastic scattering cross sections at energies near the barrier. When analyzing elastic scattering angular distributions with the standard optical model over a range of energies from slightly below to well above the Coulomb barrier one has to incorporate those effects by introducing an energy-dependent polarization potential. In a fully dynamical calculation, which explicitly allows for the excitation of the nuclear degrees of freedom, one would hope that the energy dependence of the elastic scattering cross section could be obtained automatically, via the bare, energy-independent ion–ion interaction. It is therefore of great interest to have elastic scattering data for rather heavy systems where the enhanced low-energy fusion cross sections indicate that dynamical effects are quite large.

This is the background and the motivation of our elastic scattering experiment for $^{58}$Ni + $^{64}$Ni, whose results are presented in this letter. The modified version of the kinematic coincidences technique which

[1] On leave from Institute of Atomic Energy, Beijing, China.
[2] On leave from University of Sevilla, Sevilla, Spain.
[3] On leave from Tandem Accelerator Centre, Tsukuba, Japan.
[4] On leave from Nuclear Science Centre, JNU Old Campus, New Delhi, India.
[5] On leave from Laboratorio TANDAR, CNEA, Buenos Aires, Argentina.

made these measurements possible will be described in detail in a paper under preparation.

The measurements were performed at Legnaro where the XTU Tandem accelerator provided $^{58}$Ni beams at $E_{lab}$ = 183.3, 190.7 and 204.1 MeV, with intensities in the range of 5–15 pnA. The two higher energies were chosen to match the already existing data [3] for elastic plus inelastic scattering and for quasi-elastic transfer. The experiments were done in the sliding seal scattering chamber of the laboratory; the targets were 18–35 μg/cm$^2$ evaporations of metallic $^{64}$Ni (enriched to 96.7%) on 20 μg/cm$^2$ carbon backings. The nickel-evaporated region had a rectangular shape (strip target), 1 mm wide in the reaction plane defined by the detectors. This was required by the need to sharply limit the effective beam spot size when correcting for the strong kinematic shifts of the nearly symmetric reaction partners by measuring the scattering angles of both fragments. In fact, in order to measure pure elastic scattering the experimental difficulties which we faced were manifold: besides the strong kinematic shifts (typically 3 MeV/deg in the laboratory frame), one needed to have good mass, nuclear charge and energy resolutions.

All this could be achieved by using a kinematic coincidence set-up: either the scattered beam ion or the target recoil were detected in a position sensitive silicon detector (PSSD) 8 mm×47 mm placed within the scattering chamber at 220 mm from the target. The energy and scattering angle $\theta_2$ of the impinging particle were thus measured. The collision partner was detected in a counter telescope consisting of two micro-channel plate detectors (25 mm and 50 mm in diameter), 150 cm apart from each other, which measured the time of flight (TOF) of the ion; they were followed by an ionization chamber with a transverse electric field and a split anode, capable of measuring the energy $E$ and energy loss $\Delta E$ of the ionizing particle as well as its position which determined the scattering angle $\theta_1$. The position information was derived by a measurement of the electrons drift time inside the gas, taking the start signal from the micro-channel plate detector closer to the ionization chamber and the stop signal from the anode.

The ionization chamber, originally constructed in Munich [5], had a thin ($\simeq$60 μg/cm$^2$) polypropilene window 60 mm in diameter and was operated with pure methane (99.99%) at pressures in the range 100–180 mb. The window diameter determined the solid angle of the whole set-up, and therefore also the maximum integration angle for the angular distributions, i.e. $\Delta\theta_{lab} = \pm 0.7°$. Proper normalization between the different runs was insured by two monitor detectors placed at $\theta_{lab} = \pm 23°$ and slightly below the reaction plane.

The $\Delta E$ signal resolution ($\simeq$3%) was more than adequate to separate out the charged particle transfer, which is also known [3] to have quite small cross sections around the barrier. The best mass resolution was achieved by constructing mass spectra with the formulae

$$M_1 = \mathrm{TOF}\,\frac{P_0 \sin(\theta_2)}{S_1 \sin(\theta_1+\theta_2)}\,,$$

$$M_2 = (58+64) - M_1\,,$$

that make use of TOF and of the two scattering angles; $P_0$ is the beam linear momentum and $S_1$ is the flight path. It is worthwhile to point out that we have a linear dependence of the mass on TOF, and that we do not rely on energy measurements. These features are very helpful for obtaining good mass resolution.

The TOF intrinsic resolution was around 450 ps FWHM, mainly due to the larger micro-channel plate detector. The accuracy of the measurement of scattering angles was determined by the effective 1 mm beam spot in the case of the PSSD ($\Delta\theta_2 \simeq 0.25°$), and by the position resolution ($\simeq$2 mm FWHM) in the case of the ionization chamber which was placed at an overall distance of about 2.5 m from the target ($\Delta\theta_1 \simeq 0.07°$). Fig. 1a shows an example of a mass spectrum. The peaks at $A=58$ and $A=64$ are due to beam scattering and target recoil, respectively, so that from each angular setting of the detectors we could extract data for two center of mass angles of the scattering. Smaller peaks at $A=63$, 62 are also visible, corresponding to one- and two-neutron transfer. The mass resolution is very good, being $\Delta A/A \sim 1/120$ FWHM in this case.

By gating on mass peaks, and using again the scattering angles, we constructed $Q$-value spectra (fig. 1b), i.e.

$$Q = \frac{M_0 E_0}{\sin^2(\theta_1+\theta_2)}\left(\frac{\sin^2(\theta_2)}{M_1} + \frac{\sin^2(\theta_1)}{M_2}\right) - E_0\,,$$

where $M_0$ and $E_0$ are the beam mass and energy, re-

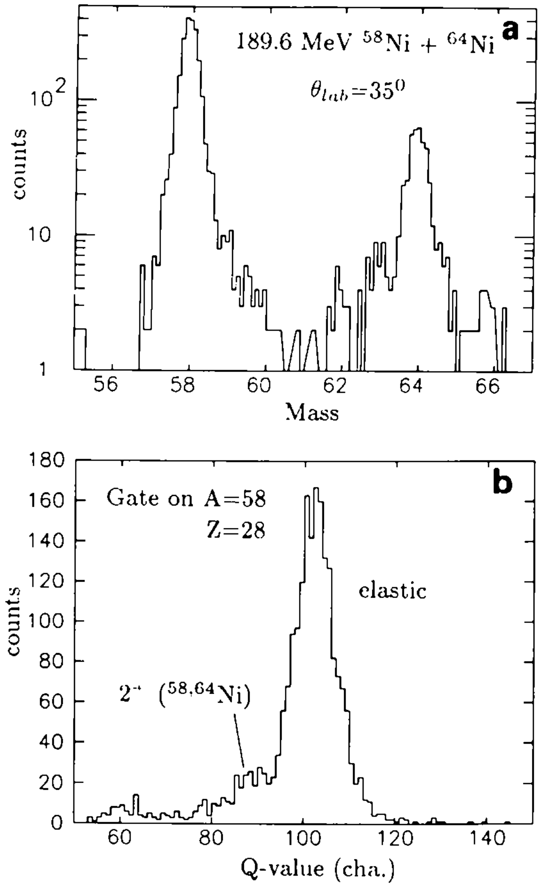


Fig. 1. Mass spectrum (a) of $Z=28$ fragments from the reaction $^{58}Ni+^{64}Ni$ at $E_{cm}=99.5$ MeV and $\theta_{lab}=35°$. $Q$-value spectrum (b) in the same conditions as above, with a gate on $A=58$ and $Z=28$; the $Q$-value axis calibration is 100 keV/channel.

spectively. In fig. 1 the $Q=0$ elastic scattering has a FWHM ~ 900 keV and it is fairly well separated from the bump at $Q\sim-1.4$ MeV arising from the excitation of the lowest $2^+$ states of both $^{58,64}Ni$, which are at $E_x=1.45$ MeV and 1.34 MeV, respectively; higher excitations are also visible. Simple gaussian fits allowed us to extract the pure elastic scattering out of such $Q$-value spectra.

The final results are shown in fig. 2, where the quoted energies are already corrected for the target thickness; the dominant contribution to the errors comes from the fits to the $Q$-value spectra. The absolute normalization of the experimental cross sections was obtained by requiring agreement at very forward angles between the data and the elastic scattering angular distribution obtained with a coupled channels Coulomb excitation calculation which included the lowest $2^+$ states of $^{58,64}Ni$ with their known electric quadrupole transition strengths. The small deviation from Rutherford scattering of the calculated forward angle elastic cross section is due to the flux loss via Coulomb excitation to the $2^+$ states. This effect does not appear if one sums the $2^+$ cross sections together with the elastic cross section. The fact that the small slope of the forward angle data follows the predictions is therefore a confirmation that pure elastic scattering has been measured.

As mentioned in the introductory part, with a coupled-channel approach we may hope to describe the energy dependence of the elastic angular distributions by using an energy independent bare ion–ion potential. This approach is also appropriate because of the strong Coulomb excitation (see above). The curves in fig. 2 are the results of coupled-channels calculations which employ ingoing wave boundary conditions inside the Coulomb barrier to account for the fusion process, contain explicit couplings to elastic excitation and transfer reaction channels, use an energy-independent real potential and have no phenomenological imaginary potentials. A full description of the calculations is given in ref. [6], where previous predictions for the $^{58}Ni+^{64}Ni$ reaction were compared to the fusion measurements and to the transfer and quasi-elastic scattering data of refs. [2,3] available at the time.

The dashed curves in fig. 2 allow for first- and second-order vibrational couplings to the one- and two-phonon states corresponding to the $2^+$ and $3^-$ excitations of the projectile and target (see also ref. [7]). The solid curves include, in addition, couplings to one- and two-neutron transfer channels (as in ref. [6]). Actually, essentially all of the difference between the two sets of calculated cross sections is due to the one-neutron transfer channels.

It is seen in fig. 2 that the overall agreement between the full calculations and our elastic scattering data is quite good (please note the linear scale). It is also apparent that the one-neutron transfer couplings are essential to obtain a reasonable agreement with the data. There is, however, an indication at all three energies and particularly at the lowest energy, that the calculations overestimate the effect of the single neutron transfer couplings. At the lowest energy, on the

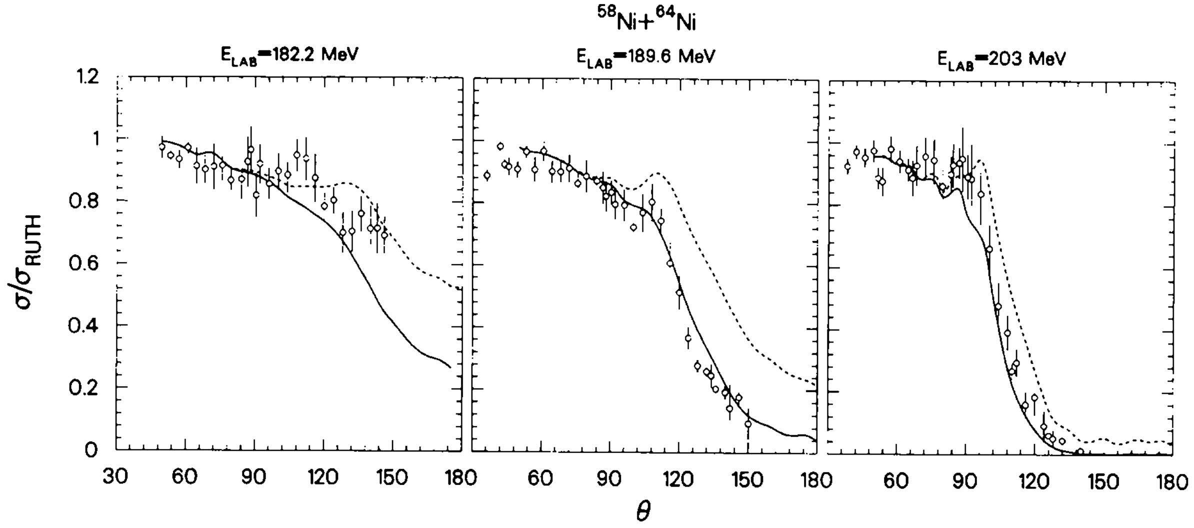


Fig. 2. Elastic scattering angular distributions for $^{58}$Ni + $^{64}$Ni at the three indicated energies. The lines are the results of the coupled-channels calculations discussed in the text.

other hand, the experimental uncertainties are larger.

The present calculations for $^{58}$Ni + $^{64}$Ni differ from the previous ones in ref. [6] by using larger nuclear deformation parameters. This change was not introduced to fit our elastic scattering data. It was based on a very recent analysis of elastic and inelastic $^{16}$O + $^{58,64}$Ni scattering data which was carried out [8] after the $^{58}$Ni + $^{64}$Ni calculations of ref. [6]. It was found that the nuclear inelastic deformation parameters, which were previously taken from the literature, had to be increased by about 18% to agree with the $^{16}$O + $^{58,64}$Ni measurements. The calculations [6,7] for the $^{58}$Ni + $^{58,64}$Ni and $^{64}$Ni + $^{64}$Ni systems have been repeated with the new deformations and a significant improvement was obtained in the low energy fusion cross sections. These new fusion results for the three combinations of nickel isotopes are shown in fig. 3 in comparison with the data [1].

For the $^{58}$Ni + $^{64}$Ni case are shown in fig. 3 two sets of fusion results corresponding to the same calculations for the elastic scattering shown in fig. 2. The dashed line refers to a calculation where only couplings to inelastic channels have been taken into account, while the full line refers to a calculation which also includes particle transfer channels. It is interesting to point out that whereas the main difference between the two sets of elastic scattering calculations in fig. 2 is due to the one-neutron transfer couplings, it is the direct two-neutron transfer couplings that account for the main difference between the two

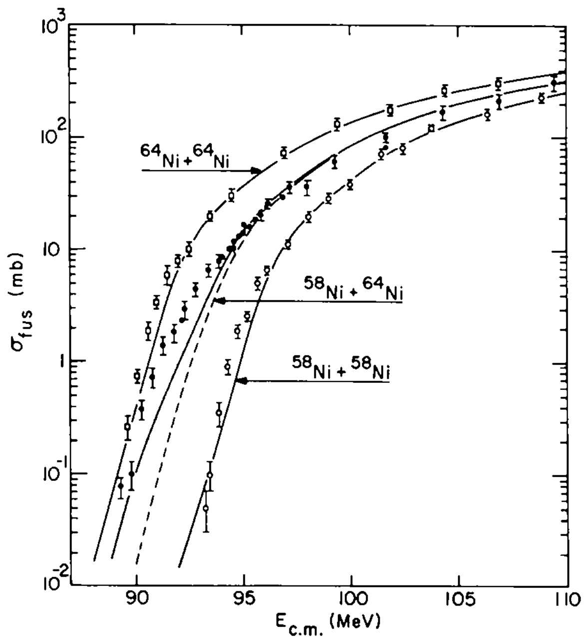


Fig. 3. Experimental fusion excitation functions for $^{58}$Ni + $^{58,64}$Ni and $^{64}$Ni + $^{64}$Ni from ref. [1] compared with the coupled-channels calculations discussed in the text.

$^{58}Ni + ^{64}Ni$ fusion calculations in the energy range below about $E_{cm} = 92$ MeV. This range is actually lower than the energies where the elastic scattering has been measured.

In summary, we have measured pure elastic scattering cross sections for $^{58}Ni + ^{64}Ni$ at three energies near the Coulomb barrier, and have analysed our data with coupled channel calculations. It is very satisfying to see that a single calculation gives a good overall account of both the elastic scattering cross sections presented here and the available fusion cross sections, without relying on adjustable parameters. Having the correct elastic cross section means that the total cross section is accounted for. Since the fusion cross section is also obtained, it may be concluded that the explicitly couplings correctly describe the bulk of the direct reaction cross sections (for detailed comparisons, see ref. [6]). Thus we see a very encouraging result in that the model gives a good account of the reaction dynamics in the $^{58}Ni + ^{64}Ni$ collision.

Grateful thanks are due to Mr. A. Dal Bello for his skillful technical assistance during the experiments, to the staff of the Legnaro Tandem accelerator, to A. Tivelli for performing part of the data analysis, and to S.J. Skorka and his group for making it possible for us to use the Munich ionization chamber. Two of the authors (H.E.) and (S.L.) are supported by the US Department of Energy, Nuclear Physics Division under contract W-31-109-ENG-38.

## References

[1] M. Beckerman et al., Phys. Rev. Lett. 45 (1980) 1472.
[2] J. Wiggins et al., Phys. Rev. C 31 (1985) 1315.
[3] K.E. Rehm et al., Phys. Rev. Lett. 55 (1985) 280.
[4] M.A. Nagarajan et al., Phys. Rev. Lett. 54 (1985) 1136; J.S. Lilley et al., Phys. Lett. B 151 (1985) 181; B. Bilwes et al., Nucl. Phys. A 473 (1987) 353.
[5] U. Quade et al., Nucl. Instrum. Methods 164 (1979) 435; K. Rudolph et al., Nucl. Instrum. Methods 204 (1983) 407.
[6] H. Esbensen and S. Landowne, Nucl. Phys. A 492 (1989) 473.
[7] H. Esbensen and S. Landowne, Phys. Rev. C 35 (1987) 2090.
[8] H. Esbensen and F. Videbaek, Phys. Rev. C 40 (1989) 126.